Journal of Solid State Chemistry 184 (2011) 1688–1694

Contents lists available at ScienceDirect

Journal of Solid State Chemistry

journal homepage: www.elsevier.com/locate/jssc

In situ variable temperature X-ray diffraction studies on the transformations of nano-precursors to La–Ni–O phases

Xiaole Weng [a], Jonathan C. Knowles [b,c], Isaac Abrahams [d], Zhongbiao Wu [a], Jawwad A. Darr [e,*]

[a] Department of Environmental Engineering, Zhejiang University; Zhejiang Provincial Engineering Research Center of Industrial Boiler & Furnace Flue Gas Pollution Control, Hangzhou 310027, PR China
[b] Division of Biomaterials and Tissue Engineering, UCL Eastman Dental Institute, University College London, 256 Gray's Inn Road, London WC1X 8LD, UK
[c] WCU Research Centre of Nanobiomedical Science, Dankook University, San#29, Anseo-dong, Dongnam-gu, Cheonan-si, Chungnam 330-714, South Korea
[d] Centre for Materials Research, School of Biological and Chemical Sciences, Queen Mary University of London, Mile End Road, London E1 4NS, UK
[e] Department of Chemistry, University College London, Christopher Ingold Laboratories, 20 Gordon Street, London WC1H 0AJ, UK

ARTICLE INFO

Article history:
Received 17 February 2011
Received in revised form
15 April 2011
Accepted 17 April 2011
Available online 4 May 2011

Keywords:
Powders-solid state reaction
La–Ni–O oxides
X-ray methods
Perovskites
Fuel cells

ABSTRACT

In situ variable temperature XRD (VT-XRD) measurements on the transformation of nano-precursors to La–Ni–O phases are presented. Experimental results showed that $LaNiO_3$ and La_2NiO_4 phases were formed at *ca.* 700 °C *via* the reaction of La_2O_3 and NiO (from the initial nano-precursors), where a relatively low temperature of 700 °C was found for the synthesis of La_2NiO_4. The formation of $La_3Ni_2O_7$ at higher temperature (up to 1150 °C) appeared to proceed through a further reaction of La_2NiO_4 with unreacted NiO, whilst the formation of $La_4Ni_3O_{10}$ (at 1075 °C) proceeded *via* a further decomposition of $LaNiO_3$. Although phase pure $La_3Ni_2O_7$ and $La_4Ni_3O_{10}$ were not directly obtained under the processing conditions herein, the results of this study allow for a better understanding of formation pathways, particularly for the higher order La–Ni–O phases.

1. Introduction

The structures of lanthanum nickel oxides, with the general formula $La_{n+1}Ni_nO_{3n+1}$, are essentially those of a Ruddlesden–Popper (RP) series [1] and are described by stacking along the *c*-axis of *n* finite $LaNiO_3$ perovskite layers separated by LaO rocksalt-like layers [2]. The processing conditions used in the synthesis of La–Ni–O phases are of considerable interest, as these can affect their properties as cathode materials in intermediate-temperature solid oxide fuel cells (IT-SOFCs) [3–12]. For the successful preparation of these phases with high purity, it is useful to understand the mechanisms under which phase formation occurs, since it is well known that phase pure syntheses of higher members of the $La_{n+1}Ni_nO_{3n+1}$ series, particularly for $n=2$ and 3 compounds (corresponding to the formulae $La_3Ni_2O_7$ and $La_4Ni_3O_{10}$, respectively), are laborious and difficult, normally requiring prolonged heating (several days) and energy intensive re-homogenization procedures [4,13–18]. There are only limited reports on thermodynamic data for the La–Ni–O system [13,19–23] and to the best of our knowledge, there are no real-time *in situ* thermodynamic analytical studies of these compounds.

In a previous report, we described the direct syntheses of $La_4Ni_3O_{10}$ and $La_3Ni_2O_7$, *via* one step heat-treatments in a muffle furnace in air (*ca.* 12 h) of the corresponding intimately mixed nano-precursors of $La(OH)_3$ and $Ni(OH)_2$ [24]. Thereafter, we reported the direct syntheses of $n=1$ and ∞ compounds, which correspond to the formulae La_2NiO_4 and $LaNiO_3$, respectively, using a similar route, although it is noted that these materials are relatively easy to access via conventional synthesis methods [25]. The nano-precursors used in these studies were synthesized using a continuous hydrothermal flow synthesis (CHFS) system [24]. CHFS or similar reactors have been used to rapidly and efficiently produce numerous inorganic metal oxide nanoparticles from pre-mixed metal salt solutions, which can rapidly be co-precipitated as homogeneously mixed oxides or solid solutions when mixed with a flow of supercritical water (which is typically at >400 °C and >22 MPa). Further details of this process are given elsewhere [26–36].

Currently, *in situ* VT-XRD has been extensively employed to study the formation or characterization of $PbTiO_3$ [37], $BaTiO_3$ [37], calcium phosphate [38], hydroxyapatite (HA) [39,40], sodium yttrium fluoride [41], γ-Bi_2MoO_6 [42], $CoAl_2O_4$ [42], silicon nitride compounds [43], and others. This technique offers an opportunity to follow thermodynamic phase changes at elevated temperatures.

Abbreviations: VT-XRD, variable temperature X-ray powder diffraction; CHFS, continuous hydrothermal flow synthesis

* Corresponding author.
E-mail address: j.a.darr@ucl.ac.uk (J.A. Darr).

0022-4596/$ - see front matter © 2011 Elsevier Inc. All rights reserved.
doi:10.1016/j.jssc.2011.04.031

In the present work, we describe the utilization of VT-XRD to follow the transformation of different nano-precursors (made via CHFS) to La–Ni–O phases under dynamic heating in order to elucidate possible reaction pathways for their formation.

2. Materials and methods

2.1. Nano-precursor synthesis

The powders were prepared using a continuous hydrothermal flow synthesis (CHFS) system as described elsewhere [26–36]. The as-prepared powders were mixtures of $La(OH)_3$ and $Ni(OH)_2$ nanoparticles with La/Ni metal ion ratios of 1:1, 2:1, 3:2 and 4:3. These powders were intimate mixtures of hexagon plate-like nickel hydroxides (*ca.* 80 nm in diameter) and needle-like lanthanum hydroxides (*ca.* 40×10 nm) [25]. Metal analysis showed that the actual lanthanum and nickel ratios of these powders were 0.96:1, 1.94:1, 2.92:2 and 3.90:3, respectively [25].

2.2. Variable temperature XRD characterization

Experiments were performed using a Bruker D8 Advance diffractometer with Ni filtered Cu-$K\alpha$ radiation and a Lynx Eye detector. To perform the high temperature experiments, an Anton Paar HTK16 heating stage with an Anton Paar TCU 2000 control unit was used, integrated with the Bruker control software. The as-prepared powders were loaded onto a platinum heater stage. The heating temperature was monitored by a type R thermocouple, which was welded to the bottom of the platinum heater strip (temperature accuracy was controlled within ± 1 K). The platinum heater enclosure was sealed and purged with either nitrogen or air at a flow rate of 2 mL min^{-1}. The sample was heated continuously at a rate of 10 °C min^{-1} up to a maximum of 1150 °C (see Table 1). During heating, data were collected over the 2θ range 25–50°, with a step size of 0.02° and a count time of 0.1 s. The sample was held at the target temperature for upto 12 h (depending on the sample). During this hold time, the sample temperature was kept constant and the delay between each complete data collection was 472 s, using the same collection parameters as above. For the attempted synthesis of $La_4Ni_3O_{10}$ (experiment 6), a slightly different regime was used. The hold temperature used was 1075 °C and better quality data was collected at this temperature using a count time of 0.5 s and a delay time between each data collection at the hold temperature of 300 s. The resultant products in each experiment were all subjected to a room-temperature scan over the 2θ range 10–120° with a step size of 0.02° and a count time of 0.1 s, which were used for Rietveld refinement using GSAS [44] for phase identification and unit cell parameter refinement. *Note*: these materials are very sensitive to partial pressure of oxygen; hence, phase transformations under direct Pt strip heating (such as that in the HTK16) may result in slight differences in phase behavior compared to that obtained in a muffle furnace as used in previous studies.

3. Results and discussion

3.1. Attempt to synthesize $LaNiO_3$ compound

The heating conditions used for the synthesis of $LaNiO_3$ *via* VT-XRD were based on our previous experimental results [25], which suggested that phase pure $LaNiO_3$ could be obtained after heat-treatment of the as-prepared powder (with 1:1 La/Ni ratio of the hydroxides) at 750 °C for 6 h in static air in an electric muffle furnace. Fig. 1 shows the evolution of the X-ray diffraction patterns (experiment 1 as shown in Table 1). At low temperatures the XRD patterns show characteristic peaks corresponding to the hydroxide precursors $La(OH)_3$ (JCPDS pattern 36-1481) and $Ni(OH)_2$ (JCPDS pattern 14-011), although those for $Ni(OH)_2$ are rather weak reflecting the poorer X-ray scattering of this phase compared to $La(OH)_3$. Peaks at *ca.* $2\theta = 40.1°$ and 46.1° are due to the Pt heating strip. Thermal expansion of the lattice parameters was observed, with peaks shifting to lower 2θ values with increasing temperature. With increasing temperature, a decrease in intensity of the precursor peaks was generally observed, which were no longer evident at *ca.* 371 °C. Interestingly, between 371 and 717 °C, only peaks attributable to the Pt substrate were observed and at 717 °C, peaks attributable to the product $LaNiO_3$ (JCPDS pattern 34-1028) appeared (XRD characteristic peaks at 2θ values *ca.* 32.6°, 40.6° and 46.9°). The presumed condensation of

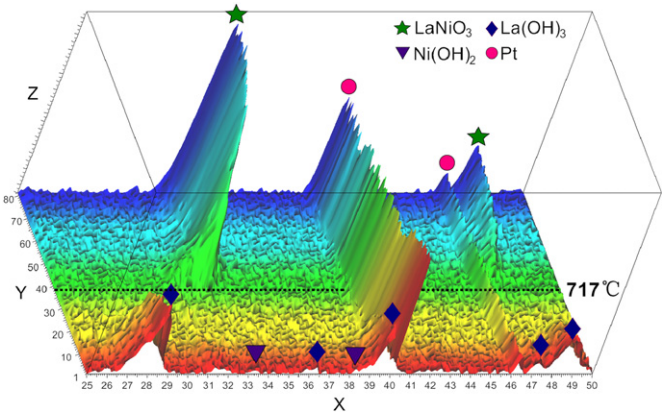

Fig. 1. 3D stacked VT-XRD patterns for the synthesis of $LaNiO_3$ *via* heat-treatment in air of nano-precursors (with 1:1 La/Ni ratio) at 750 °C for 6 h; where *x*, *y*, and *z* axes represent the 2θ scan range, scan number (corresponding to heating times) and peak intensity, respectively.

Table 1
Details of heat-treatments in VT-XRD used for experiments 1–7, showing the products identified by XRD data.

Expt.	Target phases	Total heating (time/h)	Heating temperature (°C)	Gas	Intermediate phases	Products	Comment
1	$LaNiO_3$	6	750	Air	–	$LaNiO_3$	[c]
2	La_2NiO_4	6	1000	Air	–	La_2NiO_4[a] La_2O_3 $La_3Ni_2O_7$	[d]
3	La_2NiO_4	3	700	Air	–	La_2NiO_4	[c]
4	La_2NiO_4	3	700	Argon	–	La_2NiO_4	[c]
5	$La_3Ni_2O_7$	12	1150	Air	La_2NiO_4 [b]	La_2NiO_4 $La_3Ni_2O_{7-\delta}$[a]	[d]
6	$La_4Ni_3O_{10}$	12	1075	Air	$LaNiO_3$ [b]	$LaNiO_3$ $La_4Ni_3O_{10-\delta}$[a]	[d]
7	$La_4Ni_3O_{10}$	4	1075	None	$LaNiO_3$ [b]	$La_6Ni_5O_{16}$ [a] or $La_4Ni_3O_{10-\delta}$[a] $LaNiO_3$	[d]

[a] Major phase of mixture as observed in XRD data.
[b] No NiO was observed in XRD pattern but its presence is inferred from the reagent stoichiometry and other lanthanum-containing phases identified.
[c] Results were consistent with furnace heating.
[d] Results were different to those obtained via muffle furnace heating.

the hydroxides with increasing temperature would be expected to yield La_2O_3 and NiO. The absence of Bragg peaks associated with these phases or indeed any others, suggested that at these intermediate temperatures the mixture was poorly crystalline and might indeed be amorphous. Above 717 °C, $LaNiO_3$ peaks grew in intensity as the temperature increased up to the holding temperature of 750 °C. After *ca.* 4 h at 750 °C, no further significant changes in intensity were observed suggesting completion of the reaction.

3.2. Attempted direct synthesis of La_2NiO_4

Based on our previous study on the direct synthesis of La_2NiO_4 in an electric muffle furnace [25], a target temperature of 1000 °C and a holding time of 6 h were used for the *in situ* VT-XRD experiment (experiment 2, Fig. 2). As before, peaks corresponding to the individual hydroxide precursors were evident up to around 357 °C which disappeared to be replaced by a poorly crystalline or amorphous mixture. At *ca.* 663 °C, characteristic peaks of La_2NiO_4 (similar to JCPDS pattern 36-1481) first appeared, with peak intensities increasing with increasing temperature. At *ca.* 833 °C, a peak appeared at *ca.* 29.6°, which is attributable to La_2O_3. The intensity of this peak increased with increasing temperature up to the holding temperature of 1000 °C. After *ca.* 1 h at the holding temperature, a new peak (2θ = *ca.* 31.78°) was clearly seen, which persisted on further heating at this temperature. It is believed that this peak is associated with the formation of a higher order lanthanum nickelate, probably $La_3Ni_2O_7$ (JCPDS pattern 35-1243) resulting from a reaction between La_2NiO_4 and NiO (unseen by XRD) [19]. The presence of excess NiO would be consistent with the observation of La_2O_3 in the higher temperature diffraction patterns and might be the result of phase separation and/or incomplete reaction. This is in contrast to our previous observations using a muffle furnace, where phase pure La_2NiO_4 was obtained under a similar heating regime (albeit in a different mode of heating to the Pt strip heater where the nano-precursors are in direct contact with the heating element) [25]. The difference is attributed to the different heat treatment atmospheres in the case of the Pt heater, which will be discussed later.

Experiment 2 revealed, La_2NiO_4 could be obtained at *ca.* 663 °C in air, which was significantly lower than suggested by our earlier studies (synthesis temperature of *ca.* 1000 °C [25]). Therefore, experiment 3 investigated the synthesis of La_2NiO_4 at a lower temperature. A nano-co-crystalline mixture of hydroxides with a La:Ni ratio of 2:1 was heated in air as in experiment 2. However, for experiment 3, a target temperature of 700 °C was used with a hold time of 3 h. The X-ray diffraction patterns (Fig. 3) show that

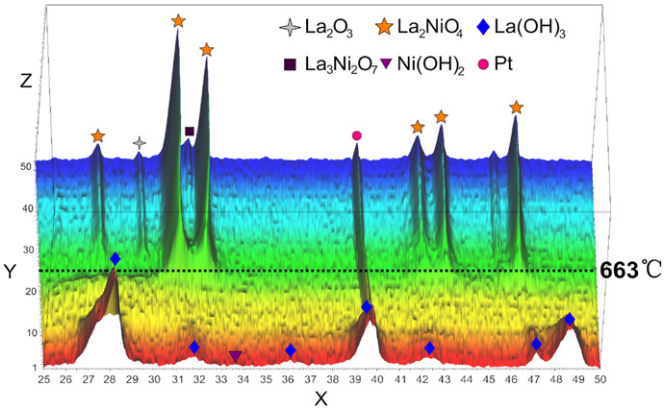

Fig. 2. 3D stacked VT-XRD patterns for the synthesis of La_2NiO_4 *via* heat-treatment in air of the nano-precursors (with 2:1 La/Ni ratio) at 1000 °C for 6 h.

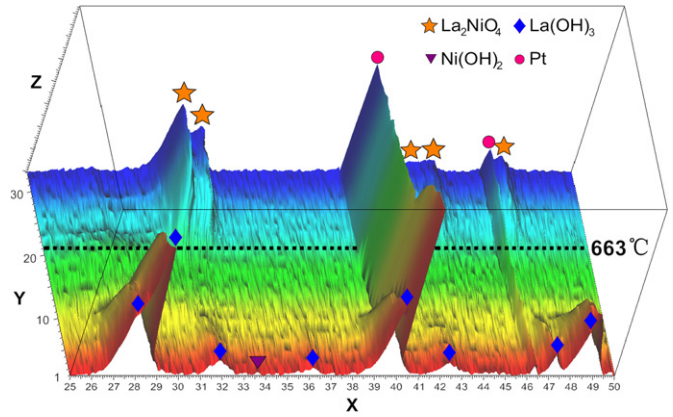

Fig. 3. 3D stacked VT-XRD patterns for the synthesis of La_2NiO_4 compound via heat-treatment in air of the nano-precursors (with 2:1 La/Ni ratio) at 700 °C for 3 h.

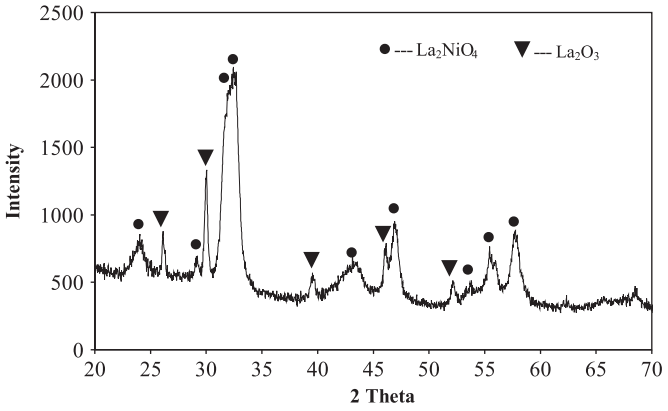

Fig. 4. XRD patterns for the synthesis of La_2NiO_4 compound via heat-treatment in air of the nano-precursors (with 2:1 La/Ni ratio) at 700 °C for 3 h in an electric muffle furnace.

crystalline peaks associated with La_2NiO_4 first appeared at *ca.* 681 °C, which is similar to experiment 2. The intensities of these peaks increased with increasing temperature (and heating time) as expected. After holding for *ca.* 3 h at 700 °C, there was no change in peak intensities, suggesting a completion of the reaction. Due to the broadness of peaks in the XRD patterns, the peaks at 2θ values of *ca.* 31.2° and 32.3° overlapped. The unit cell parameters of this tetragonal product were calculated as $a = 0.394$ nm and $c = 1.272$ nm.

A further test was conducted to simulate the experiment 3 heating regime, but in an electric muffle furnace. Heat-treatment of the identical as-prepared powders in an electric muffle furnace, at 700 °C for 3 h did not yield pure La_2NiO_4 upon cooling, with additional La_2O_3 peaks observed in the XRD pattern (Fig. 4). The observed differences between preparations *in situ* in the VT-XRD apparatus and those prepared in an electric muffle furnace are most likely due to the differences in oxygen partial pressures and/or as a result of convection originating from the different heaters, leading to differences in the relative thermodynamic stabilities of individual phases in the La–Ni–O system [19].

The synthesis of La_2NiO_4 in air is well known to yield a hyperstoichiometric compound, with a general formula $La_2NiO_{4+\delta}$ ($\delta > 0$) [7–9,45–50]; hence, a stoichiometric compound may only be obtained in an inert atmosphere (e.g. argon). It is useful to assess the effect of the incorporation of excess oxygen in La_2NiO_4 on the unit cell parameters, since this may

provide some valuable information on the structure or for any future ion conductivity pathway simulation. In light of this, in experiment 4, heat-treatment of a nano-precursor powder (from CHFS) with 2:1 La/Ni metal ratio (of the hydroxides) was carried out in argon at 700 °C for 3 h, after which, the gas was switched to air for further a 1.5 h. Fig. 5 shows the resulting X-ray diffraction patterns. Well-defined characteristic peaks of La_2NiO_4 formed as the temperature approached *ca.* 674 °C (similar to the temperature observed in experiment 3) and the reaction showed little change after *ca.* 3 h holding time (no change in peaks). Unit cell parameters of this tetragonal product were calculated at $a=0.390$ nm and $c=1.277$ nm. In contrast to experiment 3, overlapping of the peaks at 2θ values of *ca.* 31.1° and 32.5° was not observed. This was assumed to be attributed to the genuine differences in crystal structure or sintering behavior obtained in argon and air. After switching from argon to air, a sudden increase in peak intensities was observed. This is due to the lower X-ray absorption characteristics of the gas in the high temperature chamber. A small shift in peak positions to lower values was observed upon switching from argon to air. This is consistent with the incorporation of excess oxide ions to yield the hyperstoichiometric compound, $La_2NiO_{4+\delta}$, with a resulting expansion of the unit cell. Fig. 6 shows the variation of the tetragonal cell parameters *a* and *c* as a function of heating time after switching from argon to air. A slight increase of the *c* lattice parameter was observed after *ca.* 10 min heat-treatment in air and remained virtually constant thereafter. This observation is promising and supported a previous suggestion from Boehm et al. [51] that the incorporated additional oxide ions in the $La_2NiO_{4+\delta}$ phase would mainly exist in the interstitial sites between the perovskite and rock-salt layers.

In summary, from the VT-XRD results, it can be deduced that the phase changes for the syntheses of $LaNiO_3$ and La_2NiO_4 are *via* the reaction of an amorphous or ill defined intimate mixture of La_2O_3 and NiO (from initial $La(OH)_3$ and $Ni(OH)_2$ nano-precursors), which is consistent with the literature [13,19–23]. See Scheme 1.

3.3. Attempted direct synthesis of $La_3Ni_2O_7$

We previously reported the direct synthesis of phase pure $La_3Ni_2O_7$ *via* 12 h heat-treatment at 1150 °C in air, in an electric muffle furnace, of a nano-precursor powder with 3:2 La/Ni ratio of the hydroxides [24]. In light of this, experiment 5 was conducted in an attempt to synthesize and observe the formation of this material using VT-XRD (Fig. 7). The resulting XRD patterns show that on heating, La_2NiO_4 appeared when the temperature approached *ca.* 781 °C. At around 1150 °C, peaks with 2θ values at *ca.* 31.7°, 32.34°, 37.41°, 38.32°, 41.8° and 46.5° appeared and their intensities increased with time. A subsequent extended X-ray diffraction data collection carried out at room temperature on the cooled sample confirmed the presence of $La_3Ni_2O_7$, but also indicated the presence of a second phase, thought to be La_2NiO_4 (see Fig. 8). Again, possible differences in oxygen partial pressure in the VT-XRD experiment may lead to the coexistence of La_2NiO_4 and $La_3Ni_2O_7$, rather than pure $La_3Ni_2O_7$, as obtained in the electric muffle furnace under a similar heating regime. Although completely phase pure $La_3Ni_2O_7$ was not obtained, it could be concluded that the formation of $La_3Ni_2O_7$ was probably from the reaction of La_2NiO_4 and NiO (in most cases, NiO characteristic peaks were not clearly visible due to its relatively poor X-ray scattering compared to the lanthanum-containing phases), which is consistent with suggestions in the literature [13,19–23]. The phase changes observed in VT-XRD can be represented in Scheme 2.

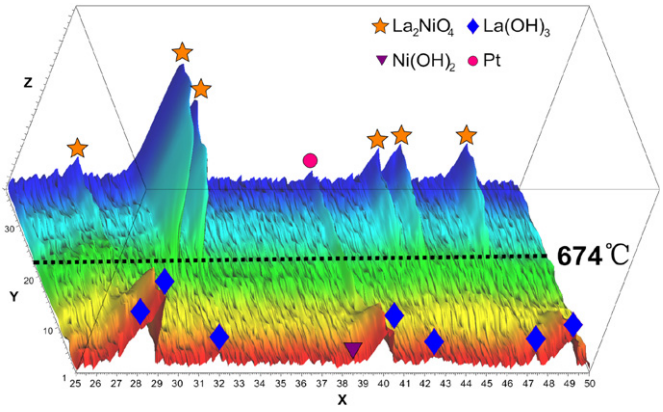

Fig. 5. 3D stacked VT-XRD patterns for the synthesis of La_2NiO_4 compound *via* heat-treatment in argon of the nano-precursors (with 2:1 La/Ni ratio) at 700 °C for 3 h.

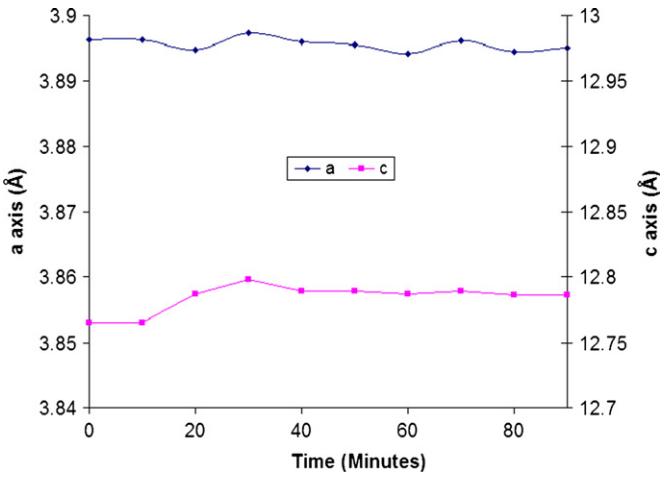

Fig. 6. Variation of *a* and *c* unit cell parameters for $La_2NiO_{4+\delta}$ made by heat-treatment of the nano-precursors (with 2:1 La/Ni ratio) at 700 °C in argon for 3 h and then subjected to a further heat-treatment in air for 1.5 h (shown above for this latter period).

$$1La(OH)_3 + 1Ni(OH)_2 \xrightarrow[\text{Amorphous}]{-2.5H_2O+0.5O} LaNiO_3$$

$$2La(OH)_3 + 1Ni(OH)_2 \xrightarrow[\text{Amorphous}]{-4H_2O} La_2NiO_4$$

Scheme 1

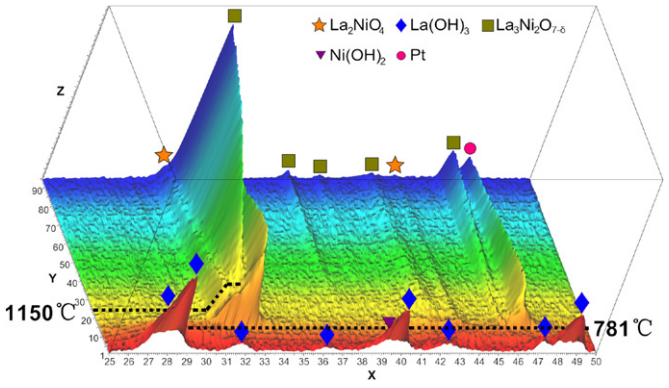

Fig. 7. 3D stacked VT-XRD patterns for the synthesis of $La_3Ni_2O_7$ *via* heat-treatment in air of the nano-precursors (with 3:2 La/Ni ratio) at 1150 °C for 12 h.

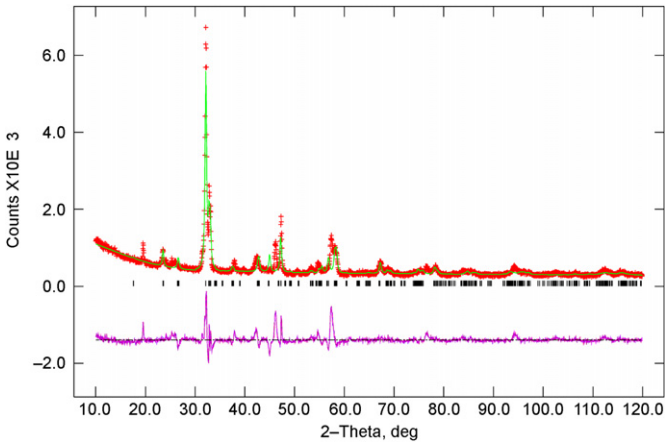

Fig. 8. Fitted X-ray diffraction profile of the sample made *via* heat-treatment in air of the nano-precursors (with 3:2 La/Ni ratio) at 1150 °C for 12 h in the VT-XRD (experiment 5). Only the major phase $La_3Ni_2O_7$ was modeled. Observed (+ signs), calculated (line) and difference (lower) profiles are shown, with reflection positions indicated by markers.

$$3La(OH)_3 + 2Ni(OH)_2 \xrightarrow[\text{Amorphous}]{-6.5H_2O} 1.5La_2NiO_4 + 0.5NiO$$

$$La_2NiO_4 + (x/3)NiO + (x/6)O_2 \rightarrow (2x/3)La_3Ni_2O_7 + (1\text{-}x)La_2NiO_4$$

Scheme 2

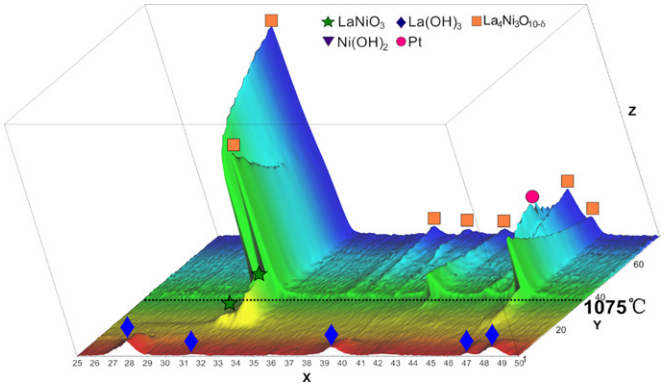

Fig. 9. 3D stacked VT-XRD patterns for the synthesis of $La_4Ni_3O_{10}$ compound via heat-treatment in air of the nano-precursors (with 4:3 La/Ni ratio) at 1075 °C for 12 h.

3.4. Attempted direct synthesis of $La_4Ni_3O_{10}$

As for $La_3Ni_2O_7$, $La_4Ni_3O_{10}$ can also be synthesized *via* heat-treatment in air of the as-prepared powder (with 4:3 La/Ni ratio of the hydroxides) at 1075 °C for 12 h in an electric muffle furnace [24]. Experiment 6 was conducted in an attempt to recreate these conditions in the VT-XRD experiment. As shown in Fig. 9, the characteristic peaks of $LaNiO_3$ appeared when the temperature approached *ca.* 719 °C and the intensities of these peaks gradually decreased with increasing heating time (and temperature). It is difficult to determine the onset decomposition temperature of the $LaNiO_3$ phase due to peak overlapping of peaks from $LaNiO_3$ and $La_4Ni_3O_{10}$ phases at 2θ values of *ca.* 32.34°, 41.36° and 46.52°. Extra peaks at 2θ values *ca.* 31.7°, 37.4°, 39.2° and 45.6° appeared when the temperature approached *ca.* 1064 °C. Again, these peaks did not perfectly fit the characteristic peaks of the $La_4Ni_3O_{10}$ phase (JCPDS pattern 35-1242) and a long X-ray data collection of the product at room temperature was conducted in order to clarify the identity of the phases present. Refinement against these data showed the product was a mixture of $La_4Ni_3O_{10}$ and $LaNiO_3$ type phases (R_{wp}=0.0797, R_p=0.0598) and their unit cell parameters were calculated as a=0.54291(7) nm, b=0.54762(7) nm, c=2.8027(4) nm and a=0.55585(9) nm, c=1.3512(4) nm, for the orthorhombic and tetragonal phases, respectively (see Fig. 10). *Note*: The sudden increase of peak intensities shown in Fig. 9 was due to the change of count time from 0.1 to 0.5 s with an aim to get better quality data collected when the temperature approached 1075 °C. In particular, the presence of $LaNiO_3$ at such a high temperature (1075 °C) suggests that the oxygen partial pressure in the VT-XRD was possibly higher than 1 bar, since this phase is known to decompose at *ca.* 850 °C under relatively lower oxygen partial pressures [19]. As such, the oxygen partial pressure in the VT-XRD experiment was significantly higher than that normally encountered in the electric muffle furnace (*ca.* 0.2 bar), which may explain the difference in the products obtained from the VT-XRD and the muffle furnace heating experiments. Again, although phase pure $La_4Ni_3O_{10}$ was not obtained on this occasion, it can be concluded that the formation of $La_4Ni_3O_{10}$ phase was initially from the decomposition of $LaNiO_3$, which was consistent with the literature [13,19–23] and the phase changes observed in VT-XRD can be represented in Scheme 3.

In addition, an extra experiment (experiment 7) was conducted to heat a 4:3 La/Ni ratio of the as-prepared powder up to 1075 °C in an unsealed VT-XRD chamber. No gas was purged through in this case. The purpose for the design of this experiment was to best simulate the airflow in an electric muffle furnace on heating, to investigate whether changes in oxygen partial pressure could result in changes in the thermodynamic stability of La–Ni–O phases as proposed above. Supplementary Figure S1 shows that $LaNiO_3$ phase appeared when the temperature approached *ca.* 725 °C, where this temperature is similar to experiment 6 (with purging air). Again, it is difficult to determine the onset decomposition temperature of $LaNiO_3$. Based on

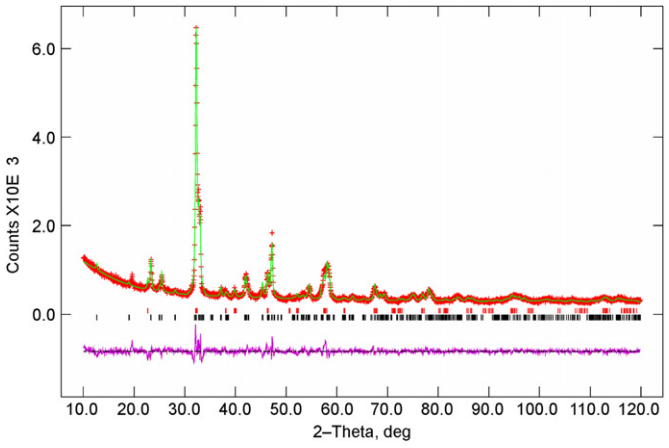

Fig. 10. Fitted X-ray diffraction profile of the sample made *via* heat-treatment in air of nano-precursors (with 4:3 La/Ni ratio) at 1075 °C for 12 h in the VT-XRD (experiment 6). Observed (+ signs), calculated (line) and difference (lower) profiles are shown with reflection positions indicated by markers $La_4Ni_3O_{10}$ (lower) and $LaNiO_3$ (upper).

$$4La(OH)_3 + 3Ni(OH)_2 \xrightarrow[\text{Amorphous}]{-9H_2O + 0.75O_2} 3LaNiO_3 + 0.5La_2O_3$$

$$LaNiO_3 + (x/6)La_2O_3 \rightarrow (x/3)La_4Ni_3O_{10} + (1\text{-}x)LaNiO_3 + (x/6)O_2$$

Scheme 3

refinement against the subsequently collected room temperature X-ray diffraction data, the product was more than likely a mixture of either $La_4Ni_3O_{10}$ or maybe even $La_6Ni_5O_{16}$ (JCPDS pattern 42-0091) and $LaNiO_3$ phases ($R_{wp}=0.0789$, $R_p=0.0591$), similar to those obtained from experiment 6. However, differences in the relative intensities of the diffraction peaks compared to those obtained in experiment 6, suggests that the differing oxygen partial pressures during synthesis, resulted in differences in the amounts and types of each phase obtained.

It was very difficult to distinguish the $La_4Ni_3O_{10}$ and possible $La_6Ni_5O_{16}$ phases from the refinement due to the similarity in the XRD patterns of these two phases. However, it should be noted that some authors have suggested that the $La_6Ni_5O_{16}$ phase might not exist and was actually either $La_4Ni_3O_{10}$ [13] or $La_3Ni_2O_7$ [19]. The $La_6Ni_5O_{16}$ phase (not in a pure form) was first reported by Kitayama in 1990 [13], which was synthesized *via* heating a La_2O_3 and NiO mixture (with the mole ratio of 10:40 and 45:55) at 1200 °C for *ca.* 55 h with intermittent mixings. The oxygen partial pressure used by the aforementioned author was at 0.68 bar, which is significantly higher than ambient oxygen partial pressure (0.2 bar). As such, if the $La_6Ni_5O_{16}$ phase was present in the mixture (resulting from experiment 7), the different oxygen partial pressures in the VT-XRD and muffle furnace would be the reason for its formation. Therefore, further analysis on the mixture is required. Nevertheless, unit cell parameters for the $La_4Ni_3O_{10}$ (or possibly $La_6Ni_5O_{16}$) and $LaNiO_3$ phases were calculated at $a=0.54240(8)$ nm, $b=0.54676(8)$ nm, $c=2.7987(5)$ nm and $a=b=0.5557(2)$ nm, $c=1.3327(6)$ nm, respectively (see Figure S2), which were slightly different from those obtained from experiment 6.

4. Conclusions

An *in situ* VT-XRD study of La/Ni hydroxide nano-precursors to several La–Ni–O phases was conducted. The syntheses of higher members of La–Ni–O series ($n=2$ and 3) was not totally consistent with previous results obtained *via* muffle furnace heating, which is likely to be due to differences in oxygen partial pressures. However, the studies were extremely illuminating and clearly suggested reaction pathways for the formation of the target compounds. As such, further optimization of oxygen partial pressure in VT-XRD experiments, making them comparable to that in a muffle furnace, will be necessary in any future work. The use of a nano-precursor route for the attempted direct synthesis of the La–Ni–O pure phases worked very well for the lower members of the La–Ni–O series ($n=1$ and ∞), in that both of these phases were formed. Notably for the synthesis of La_2NiO_4, only a 700 °C heating temperature (both in air and argon) was required, which is the lowest synthesis temperature for this phase reported so far.

Acknowledgments

The project was financially supported by Changjiang Scholar Incentive Programme (2009), Ministry of Education, PR China, China Postdoctoral Science Foundation (20100471738), Zhejiang Higher Education Scientific Research Program (Y200909610). EPSRC is thanked for funding the "Continuous Hydrothermal synthesis of Nanomaterials: from Lab to pilot plant" project EPSRC Reference: EP/E040551/1. This work was supported in part (JCK) by the WCU Program through the National Research Foundation of Korea (NRF) funded by the Ministry of Education, Science and Technology (No. R31-10069).

Appendix A. Supplementary materials

Supplementary data associated with this article can be found in the online version at doi:10.1016/j.jssc.2011.04.031.

References

[1] S.N. Ruddlesden, P. Popper, Acta Crystallogr. 11 (1958) 54.
[2] P.J. Lacorre, J. Solid State Chem. 97 (1992) 495–500.
[3] G. Amow, J. Au, I. Davidson, Solid State Ionics 177 (2006) 1837–1841.
[4] G. Amow, I.J. Davidson, S.J. Skinner, Solid State Ionics 177 (2006) 1205–1210.
[5] G. Amow, S.J. Skinner, J. Solid State Electrochem. 10 (2006) 538–546.
[6] S.J. Skinner, Int. J. Inorg. Mater. 3 (2001) 113–121.
[7] A. Aguadero, J.A. Alonso, M.J. Martinez-Lope, M.T. Fernandez-Diaz, M.J. Escudero, L. Daza, J. Mater. Chem. 16 (2006) 3402–3408.
[8] A. Demourgues, P. Dordor, J.P. Doumerc, J.C. Grenier, E. Marquestaut, M. Pouchard, A. Villesuzanne, A. Wattiaux, J. Solid State Chem. 124 (1996) 199–204.
[9] C. Li, T.H. Hu, H. Zhang, Y. Chen, J. Jin, N.R. Yang, J. Membr. Sci. 226 (2003) 1–7.
[10] C.N.R. Rao, D.J. Buttrey, N. Otsuka, P. Ganguly, H.R. Harrison, C.J. Sandberg, J.M. Honig, J. Solid State Chem. 51 (1984) 266–269.
[11] M. Sayer, P. Odier, J. Solid State Chem. 67 (1987) 26–36.
[12] D.K. Seo, W. Liang, M.H. Whangbo, Z. Zhang, M. Greenblatt, Inorg. Chem. 35 (1996) 6396–6400.
[13] K. Kitayama, J. Solid State Chem. 87 (1990) 165–172.
[14] L.A. Bendersky, M. Greenblatt, R. Chen, J. Solid State Chem. 174 (2003) 418–423.
[15] Z. Zhang, M. Greenblatt, J.B. Goodenough, J. Solid State Chem. 108 (1994) 402–409.
[16] Z. Zhang, M. Greenblatt, J Solid State Chem. 117 (1995) 236–246.
[17] C.D. Ling, D.N. Argyriou, G. Wu, J.J. Neumeier, J. Solid State Chem. 152 (2000) 517–525.
[18] K. Sreedhar, M. McElfresh, D. Perry, D. Kim, P. Metcalf, J.M. Honig, J. Solid State Chem. 110 (1994) 208–215.
[19] M. Zinkevich, F. Aldinger, J. Alloys Compd. 375 (2004) 147–161.
[20] D.O. Bannikov, V.A. Cherepanov, J. Solid State Chem. 179 (2006) 2721–2727.
[21] D.O. Bannikov, A.P. Safronov, V.A. Cherepanov, Thermochim. Acta 451 (2006) 22–26.
[22] P. Odier, Y. Nigara, J. Coutures, M. Sayer, J. Solid State Chem. 56 (1985) 32–40.
[23] V.A. Cherepanov, A.N. Petrov, L.Y. Grimova, E.M. Novitskii, Zh. Fiz. Khim. 57 (1983) 859–863.
[24] X. Weng, P. Boldrin, I. Abrahams, S.J. Skinner, J.A. Darr, Chem. Mater. 19 (2007) 4382–4384.
[25] X.L. Weng, P. Boldrin, I. Abrahams, S.J. Skinner, S. Kellici, J.A. Darr, J. Solid State Chem. 181 (2008) 1123–1132.
[26] J.A. Darr, M. Poliakoff, Abstr. Paper Am. Chem. Soc. 216 (1998) U648.
[27] Z.C. Zhang, S. Brown, J.B.M. Goodall, X.L. Weng, K. Thompson, K.N. Gong, S. Kellici, R.J.H. Clark, J.R.G. Evans, J.A. Darr, J. Alloys Compd. 476 (2009) 451–456.
[28] X.L. Weng, B. Perston, X.Z. Wang, I. Abrahams, T. Lin, S.F. Yang, J.R.G. Evans, D.J. Morgan, A.F. Carley, M. Bowker, J.C. Knowles, I. Rehman, J.A. Darr, Appl. Catal. B: Environ. 90 (2009) 405–415.
[29] X.L. Weng, J.K. Cockcroft, G. Hyett, M. Vickers, P. Boldrin, C.C. Tang, S.P. Thompson, J.E. Parker, J.C. Knowles, I. Rehman, I. Parkin, J.R.G. Evans, J.A. Darr, J. Comb. Chem. 11 (2009) 829–834.
[30] K. Thompson, J. Goodall, S. Kellici, J.A. Mattinson, T.A. Egerton, I. Rehman, J.A. Darr, J. Chem. Tech. Biot. 84 (2009) 1717–1725.
[31] V. Middelkoop, P. Boldrin, M. Peel, T. Buslaps, P. Barnes, J.A. Darr, S.D.M. Jacques, Chem. Mater. 21 (2009) 2430–2435.
[32] Z. Zhang, J.B.M. Goodall, S. Brown, L. Karlsson, R.J.H. Clark, J.L. Hutchison, I.U. Rehman, J.A. Darr, Dalton Trans. 39 (2010) 711–714.
[33] T. Lin, S. Kellici, K. Gong, K. Thompson, J.R.G. Evans, X. Wang, J.A. Darr, J. Comb. Chem. 12 (2010) 383–392.
[34] X. Weng, D. Brett, V. Yufit, P. Shearing, N. Brandon, M. Reece, H. Yan, C. Tighe, J.A. Darr, Solid State Ionics 181 (2010) 827–834.
[35] R. Gruar, C.J. Tighe, L.M. Reilly, G. Sankar, J.A. Darr, Solid State Sci. 12 (2010) 1683–1686.
[36] S. Kellici, K.A. Gong, T.A. Lin, S. Brown, R.J.H. Clark, M. Vickers, J.K. Cockcroft, V. Middelkoop, P. Barnes, J.M. Perkins, C.J. Tighe, J.A. Darr, Phil. Trans. R. Soc. A—Math. Phys. Eng. Sci. 368 (2010) 4331–4349.
[37] J. Mullens, K. Van Werde, G. Vanhoyland, R. Nouwen, M.K. Van Bael, L.C. Van Poucke, Thermochim. Acta 392–393 (2002) 29–35.
[38] A.G. Dias, J.M.S. Skakle, I.R. Gibson, M.A. Lopes, J.D. Santos, J. Non-Cryst. Solids 351 (2005) 810–817.
[39] S.W.K. Kweh, K.A. Khor, P. Cheang, Biomater. 23 (2002) 381–387.
[40] W.J. Shih, J.W. Wang, M.C. Wang, M.H. Hon, Mater. Sci. Eng. C 26 (2006) 1434–1438.
[41] M.D. Mathews, B.R. Ambekar, A.K. Tyagi, J. Kohler, J. Alloys Compd. 377 (2004) 162–166.
[42] A.M. Beale, L.M. Reilly, G. Sankar, Appl. Catal. A 325 (2007) 290–295.
[43] B. Lei, O. Babushkin, R. Warren, J. Eur. Ceram. Soc. 17 (1997) 1113–1118.

[44] A.C. Larson, R.B. Von Dreele, Los Alamos National Laboratory Report LAUR 8 (1986) 748.
[45] A. Demourgues, F. Weill, J.C. Grenier, A. Wattiaux, M. Pouchard, Physica C 192 (1992) 425–434.
[46] M.L. Fontaine, C. Laberty-Robert, M. Verelst, J. Pielaszeck, P. Lenormand, F. Ansart, P. Tailhades, Mater. Res. Bull. 41 (2006) 1747–1753.
[47] D.P. Huang, Q. Xu, F. Zhang, W. Chen, H.X. Liu, J. Zhou, Mater. Lett. 60 (2006) 1892–1895.
[48] K. Ishikawa, W. Shibata, K. Watanabe, T. Isonaga, M. Hashimoto, Y. Suzuki, J. Solid State Chem. 131 (1997) 275–281.
[49] T. Kyomen, M. Oguni, M. Itoh, K. Kitayama, Phys. Rev. B 60 (1999) 815–821.
[50] L. Minervini, R.W. Grimes, J.A. Kilner, K.E. Sickafus, J. Mater. Chem. 10 (2000) 2349–2354.
[51] E. Boehm, J.M. Bassat, P. Dordor, F. Mauvy, J.C. Grenier, 6P. Stevens, Solid State Ionics 176 (2005) 2717–2725.